



Multiphysics Modelling And Thermal Performance Of A Prototype Transformer Filled With Bio-Based Insulating Oil Under Various Load Conditions

Bédiane Brice Babeu Tchounga¹, Ghislain Mengata Mengounou², Emeric Tchamdjio Nkouetcha³, Adolphe Moukengue Imano⁴

¹ Laboratory of Technologies and Applied Science, University of Douala, BP: 7236 Douala, Cameroon, bediane2008@yahoo.fr

² Laboratory of Technologies and Applied Science, University of Douala, BP: 7236 Douala, Cameroon, megounal@yahoo.fr

³ Laboratory of Technologies and Applied Science, University of Douala, BP: 7236 Douala, Cameroon, tchamdjio@uni-douala.com

⁴ Laboratory of Technologies and Applied Science, University of Douala, BP: 7236 Douala, Cameroon, moukengue@univ-douala.com

Received Date : April 4 , 2022

Accepted Date : April 27, 2022

Published Date : May 07, 2022

ABSTRACT

Before designing and engineering an environmentally friendly immersion transformer, it is important to consider its thermal performance. Increasingly bio-based insulating oil develops as alternatives to mineral oil for transformers. The characterization of these bio-insulators by the standards for insulation for electrical materials in use is the problem. This paper provides a partial answer to this problem by presenting a numerical study based on the finite element method of the thermal performance of a prototype 3 KVA 50 Hz power transformer filled with bio-insulators for the cases of different loads. Using COMSOL Multiphysics 5.4, a multiphysics model was designed to evaluate the temperature distribution for each insulator (mineral oil (MO), castor oil methyl ester (COME), palm kernel oil methyl ester (PKOME), and palm kernel oil methyl ester plus nanoparticles of titanium (PKOME+NANO)) under various loads. To predict the temperature evolution by estimating the hot spots and to optimize the choice of the type of liquid insulation for power transformers at the scientific level, the thermal property models were integrated into COMSOL using the finite element method. We found that taking into account the temperature evolution of the hot spots in the transformer, the one filled with natural ester can resist aging more than the one filled with mineral oil for different loads. Therefore natural esters can be alternatives to mineral oil for power transformers. However, mineral oil has better thermal inertia than the natural esters in our study.

Key words: Loads, Thermal performance, Mineral oil, Multi-physics model, Natural esters.

1. INTRODUCTION

The power system is constantly subject to disturbances such as poor reliability and stability, noncontinuity of service, increasing demand, choice of technology, and life span. The power transformer represents 60% of the capital of equipment in the power system. Because of its very high cost, it requires the implementation of different means of protection to optimize its operation. This optimization process also depends on the quality of the electrical insulation systems, whether solid, liquid, or solid/liquid. Mineral oils are the most commonly used in power transformers. However, due to their nondegradable and toxic nature, there is a growing trend to replace them with bio-insulators that are degradable (>95%), less harmful to the environment, and have a high flash point (>300°C), and absorb more moisture [1].

Therefore, it is essential to consider all factors to ensure total system reliability and material optimization when designing an immersed transformer. Several works have been published on the design of transformer models, these, to emphasize on the properties of mineral and ester oils in them, and also on the analysis of thermal effects and performance in the transformer using advanced simulation calculation programs such as ANSYS (finite volume method) and COMSOL (finite element method). For example, Eleftherios et al. proposed design steps in 2008 [2]. Vasilija and Goran developed and analyzed the three-phase distribution transformer procedure in 2000, applying analytical and numerical methods. They are developing a computer program in Matlab to calculate the parameters and characteristics. It proved that the proposed design was accurate enough to implement the transformer parameters [3]. Between 2011 and 2016, several models have designing to analyze different parameters by researchers.

Fernando Delgado and al, Park, Lecuna and al, Santisteban and al developing a 3D model and a 2D model of an Oil Natural-Air Natural distribution transformer, are demonstrating the ability of the simplified 2D model to represent the thermal behavior of the whole transformer [4], [5], [6], [7]. Only a few parameters are considered insufficient for the different studies above. To overcome these, recently in 2018, Ortiz et al. developed with COMSOL a 2D numerical model to reproduce the thermal-hydraulic behavior of the samples to determine the temperature and velocity distributions of the different samples to analyze their differences, compare their cooling capacity [8]. The same year, Seeralin Nayager and Nilakanta and al developed a 3D model for thermal analysis (the material used was mineral oil and ester oil) and for the detection of the hottest point using the finite element method [9], [10]. In 2019, Kassi developed a thermo-fluidic numerical model using COMSOL Multiphysics 4.3a software used to study the impact of aging on the cooling capacity of mineral oils and PFE (high fire point) oils. He concluded that the hot spot is always in the upper part of the windings and it moves from top to bottom during aging and he also observed that depending on the temperature profile on the different axes, the maximum temperatures of the mineral oils are higher than those of the alternative oils on some winding discs [11]. In the same year, M.M.M. Salama and al designed a 3D CFD COMSOL model to calculate the top oil temperature rating and the hottest point temperature rating of the winding for environmentally friendly oils and mineral oil [12]. In 2021, Kendeg and al presents a 3D multiphysics model for temperature prediction in three types of three-phase transformers called Y-shaped, 3-column, and 5-column transformers using the finite element method for nonlinear calculation of the magnetic field associated with the circuit equations. Simulation results obtained with the COMSOL Multiphysics software show that it is possible to predict the temperature distribution in the transformer and successfully determine the hottest zone inside the transformer [13]. Starting from context and using esters developed in the laboratory to promote the use of natural resources and contribute to the manufacture of new transformer dielectrics, it is judicious to evaluate the extent to which these esters can affect the thermal performance of the transformer.

This paper proposes a multiphysics model of a power transformer using COMSOL Multiphysics 5.4 software. Using the finite element method, this allows, the evaluation of the thermal performance of the power transformer filled with natural esters palm kernel oil, palm kernel oil plus titanium nanoparticles (TiO₂), castor oil, and mineral oil, to compare them according to their behavior for different loads. Most of the works carried out used other types of natural esters for their study. This result is intend to be guide for the choice of insulation in the design of transformers, to deduce the relative ageing rate of transformers and to ensure the useful life of the transformers.

2. LOAD AND INSULATING CHARACTERISATION

2.1 Load characteristics

To observe the impact of loads on the thermal performance of the transformer for different insulators, three load cases (observed over a whole day) were considered in Table 1. Current ratings in the transformers are considered 1A in the high voltage winding (3000 V) and 13.04A in the low voltage winding (230 V). In each transformer, the ambient temperature is constant throughout the day. Observation of the temperature variation is made for each liquid insulator and as a function of the loads over the day following the IEEE Std C57.12.90-2015 transformer stabilization criteria standard [14]. Load depends on the random events that occur in the power system. Each regime is differentiated according to the value of the rated load current. The Rated regime corresponds to the period when the applied load current is equal to the value of the rated current, the long duration emergency regime corresponds to an application of load current higher than the rated value resulting in a higher stabilized temperature for a long period and the short duration emergency regime corresponds to the high load regime with a transient character for less than thirty minutes where the temperature is still higher [15].

Table 1: Winding current for each load regime

Load regime	Current flow (A)
Rated regime	13.04
Long-time emergency regime	15.02
Short-time emergency regime	17.34

2.2 Characteristics of liquid bio-based insulating (experimental result)

The esters mad with bio-based insulating available on site. Numerous studies carried out by the research team have made it possible to master the standards (ASTM D4052-96, ASTM 445, ISO 3675, ASTM D2717, and ASTM 2766) and characterization protocols for bio-based insulating such as PKOME, COME, and (PKOME+NANO) [16], [17], [18]. The properties of those environmentally friendly insulators used are dynamic viscosity, density, thermal conductivity, and specific heat capacity. These properties obtain experimentally.

A. Density

The density of liquid depends on the density ρ , which characterizes the mass of the oil per unit volume. It determines according to the requirements of ASTM D4052-96 [19]. It is determined using a balance, a syringe of precise volume, and a beaker at room temperature. The expression for ρ is given in “(1)” and for the density by “(2)”.

$$\rho \left[\frac{Kg}{m^3} \right] = \frac{m}{V} \quad (1)$$

$$Density = \frac{\rho_{liquid}}{\rho_{water}} \quad (2)$$

m: masse en Kg; V: volume en m³

B. Dynamic viscosity

Viscosity is defined as the resistance to the flow of a liquid under gravity. To ensure proper cooling, the bio-based insulating in the transformers must be of the Newtonian type. Their maximum viscosity at 40°C must be less than 12 mm²/s according to ASTM 445. The value is obtained using a viscometer with a capillary, a viscometer stand that allows the viscometer to be in the upright position, a thermostatically controlled bath, which contains water of sufficient depth, and a stopwatch to measure the time. This time is used in “(3)” to determine the viscosity [20]. The device for measuring the viscosity is shown in Figure 1.

$$\eta = k(t - c) \quad (3)$$

k: viscometer constant; t: time of oil flow between the two marks; C: kinetic energy correction



Figure 1: Device for measuring viscosity

C. Thermal conductivity

Thermal conductivity is the ability of a body to conduct heat. For insulating liquids, it is between 0.10 and 0.16 w/m°C according to ASTM D2717. Thermal conductivity determines by “(4)” which depends on the equations for the resistance power of the wire and the slope "P". The device for measuring the thermal conductivity is shown in Figure 2.

$$\lambda = Q / 4\pi P \quad (4)$$

Q (W/m): linear power of the heating wire, λ (W/m°C): thermal conductivity of the oil

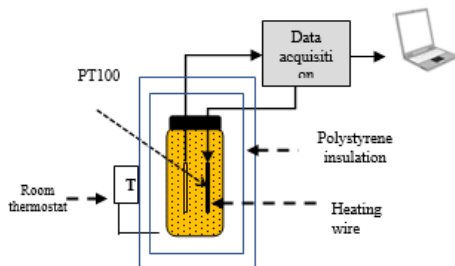


Figure 2: Device for measuring thermal conductivity

D. Specific heat capacity

Specific heat is a measurable physical quantity of the amount of heat per unit mass required to raise the temperature by one degree Celsius. It reflects the ability of a body to absorb heat and heat up. For the transformer oil, the higher the specific heat value, the less the transformer will heat up. The specific heat value for insulating liquids ranges from 1000 to 2300J/kg.K and can determine according to ASTM 2766. It is measured using a calorimeter, a DC generator, a voltmeter, and a data logging device. Figure 3 shows the experimental set-up for measuring the specific heat capacity.

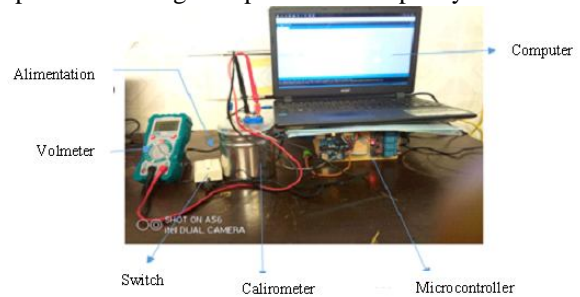


Figure 3: Experimental device for measuring specific heat

In compliance with the standards and protocols determining the physical and dielectric properties of esters, the results of the characteristic values were obtained and collected in Table 2 after experimental tests.

Table 2: Properties of dielectric insulating

Characteristics	Density	Dynamic viscosity	Thermal Conductivity	Specific Heat Capacity
Unit	Kg/m ³	mm ² /s	W/m.°C	J/Kg.K
Standard	ASTM D4052	ASTM 445	ASTM D2717	ASTM 2766
Mineral oil	0,864	9,2	0,12	2100
PKOME	0,895	4,46	0,158	2158
COME	0,871	15,06	0,129	1825
Air	1,23	18,510 ⁻⁶	400	385
PKOME + NANO	0,95	3,15	0,231	2200

3. MULTIPHYSICS MODELLING

3.1 Approach method

A 3D finite element model (FEM) of the prototype transformer, 3 KVA, 50 Hz made by COMSOL Multiphysics 5.4 software to determine the hottest points in the MO, PKOME, PKOME+NANO, and COME transformers prototypes. The values obtained are exploited using the Matlab software to observe the evolution of temperature in the prototypes, for a whole day for each load case. The methodology of the approach summarizes in the diagram below (Figure 4).

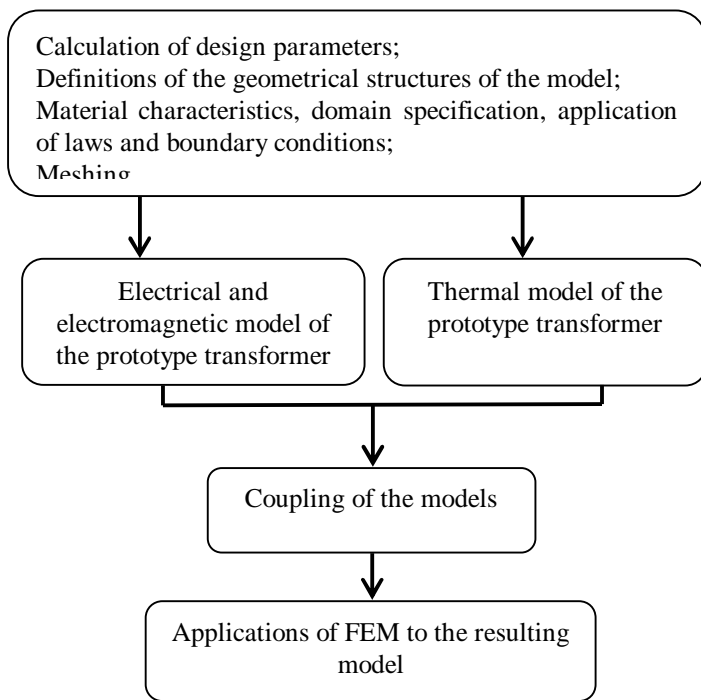


Figure 4: Diagram of the approach methodology

3.2 Tools used and meshing

The tools or materials needed for the modeling are those used in practice in the transformer. The properties of the different components give in Table 3. They are solid insulation (paper), windings (copper), oil tank (steel), magnetic circuit (mild steel), and metal components (iron).

Table 3: Material properties [21] [22]

Component	Coil	Core	Reservoir	Solid insulation
Material	Copper	Soft iron	Steel	Paper
Thermal conductivity (W/m.°K)	400	71,10	76.2	0,19
Density (Kg/m3)	8700	7850	7850	930
Specific heat capacity (J/Kg.°K)	385	464.57	440	1340
Relative permeability	1	1	600	2,8
Electrical conductivity (S/m)	6×10^7	0.1	$1,12 \times 10^7$	10^{-15}

The physical model and geometry of the studied transformer after meshing are presented in Figure 5, which shows the magnetic circuit and windings (Figure 5 (a)) and the complete model (Figure 5 (b)). The mesh is used for solving numerical problems by the finite element method. The structure of the

mesh depends on the quality of the finite elements. Here the mesh adapted for the different coolants is used.

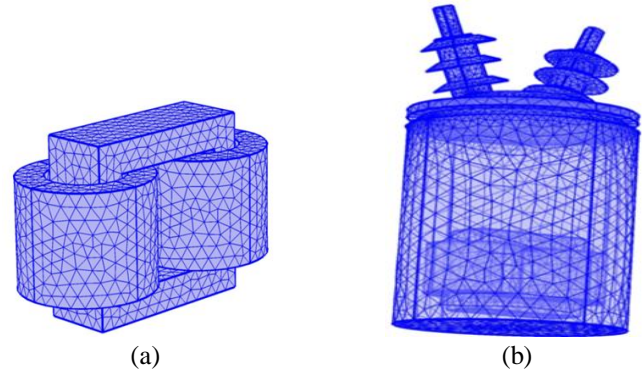


Figure 5: Physical model after meshing: (a) magnetic circuit and windings; (b) complete model

3.3 Validated model

3.3.1. Electromagnetic model

The electromagnetic model used for the description of the laws and formalism of the interaction between electromagnetic waves and material. Laws are governing by the Maxwell-Farraday, Ampere, and Fourier equations in heat conduction [23]. The boundary conditions considered have no electrical connection between the primary and the secondary; unsaturated magnetic circuit. Equations (5) govern the electromagnetic field of the coils when they are operating in AC.

$$\begin{cases} \nabla \times \vec{A} = \vec{B}; \vec{E} = -j\omega\vec{A}; \vec{B} = \mu\vec{H}; \vec{J} = \sigma\vec{E} \\ -\omega^2\gamma\vec{A} + j\omega\sigma\vec{A} + \nabla \times (\mu^{-1}\nabla \times \vec{A}) = 0 \end{cases} \quad (5)$$

\vec{A} : magnetic potential vector in Wb/m; B: magnetising field strength in T; E: electric field strength in N/C; \vec{H} : magnetic field strength in A/m; \vec{J} : current density in A/m²; j: imaginary unit; ω : phase shift angle equal to $2\pi f$; f: frequency at 50 Hz; γ : dielectric constant in F/M; μ : magnetic permeability in H/m; σ : electrical conductivity in S/m.

The equations are supplemented by the constitutive relations of the materials and the flow conditions that govern the correlation between the electric and magnetic fields on the surfaces of the materials (wooden component and oil tank). Equation (6) is given by the software.

$$\sqrt{\frac{\mu_0\mu_r}{\gamma_0\gamma_r - j(\sigma/\omega)}} \vec{n} \times \vec{H} + \vec{E} - (\vec{n} - \vec{E})\vec{n} = (\vec{n} \cdot \vec{E}_s)\vec{n} - \vec{E}_s \quad (6)$$

E: electric field strength of the tangential component; n: normal vector on the conducting surfaces; μ_0 : relative permeability of vacuum at $4\pi \times 10^{-7}$ H/m; μ_r : relative permeability; γ_0 : dielectric constant of vacuum $10^{-9}/36\pi$ F/m; γ_r : relative dielectric constant.

3.4.2. Thermal model

Heat exchange in this transformer model is due to natural convection (conduction between two media, at least one of which is a moving fluid). The heat transfer in solids must be different from the heat transfer in fluids because the heat source results from the volume of electromagnetic and Joule losses in the primary and secondary windings responsible for the temperature in the transformer tank [13].

The heat transfer on the external surface of the oil tank is considered to be natural convection with air so the relationship is given by “(7)”.

$$-q = h(T_{env} - T) \quad (7)$$

q: heat flux density in W/m²; h: external heat transfer coefficient in W/(m² .K) ; T_{env}: temperature in 293.15 K.

The heat transfer equation developed using the first law of thermodynamics is the default equation in COMSOL [23]. All terms and coefficients related to heat transfer are included in this default equation. Its mathematical formulation is given by:

$$\rho c_p (\partial T / \partial t + (u \nabla) T) = -\nabla q + \tau : S - T / \rho \partial p / \partial t_p (\partial p / \partial t + (u \nabla) p) + q''' \quad (8)$$

ρ: density (kg/m³); C_p: specific heat capacity at constant pressure (J/(kg.K)); T: absolute temperature (K); u: velocity vector (m/s); q: conductive heat flux (W/m²); p: pressure (Pa); τ: viscous stress tensor (Pa); S: strain rate tensor (1/s); q''': heat sources other than viscous heating (W/m³); k: spatially dependent or independent.

4. SIMULATION RESULTS AND DISCUSSION

4.1 Magnetic fields

Figure 6 shows the magnetic flux density and magnetic flux flow in the windings and core. It allows us to validate the choice of winding, the size, and the characteristics of the magnetic circuit.

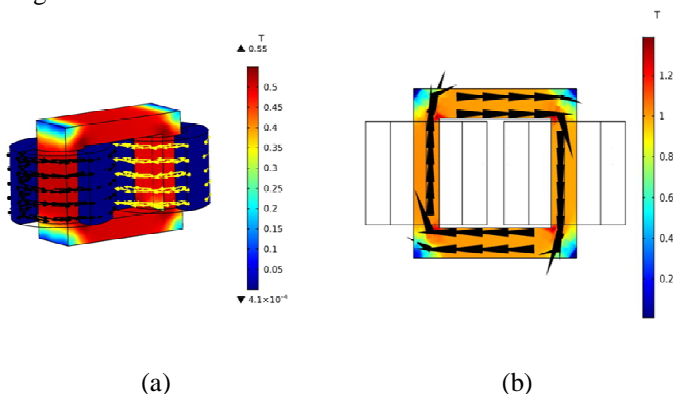


Figure 6: (a) Magnetic flux density and current in the windings; (b) Magnetic flux density in the core

We see that the flux created by the sinusoidal AC voltage is channeled and also that the maximum value of the magnetic flux is around 1.2 Tesla. This result is in line with that of Kendeg in 2021 concerning the channeling of magnetic flux.

4.2 Evolution of temperature in insulators for various loads

The temperature distributions as a function of loadings for air, mineral oil (MO), COME, PKOME, and PKOME+NANO are shown in Figures 7, 8, and 9.

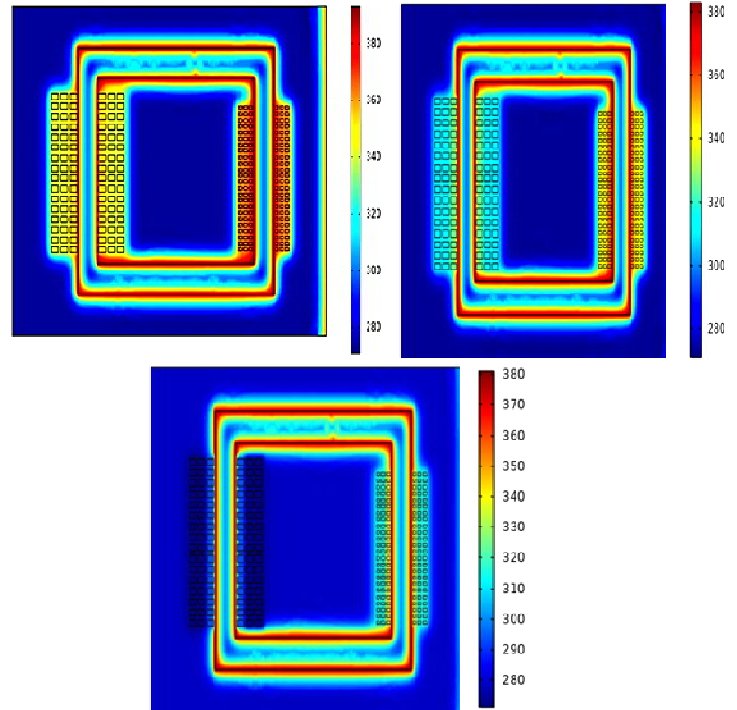


Figure 7: Temperature of hot spots in rated regime for: (a) air; (b) MO; (c) COME; (d) PKOME

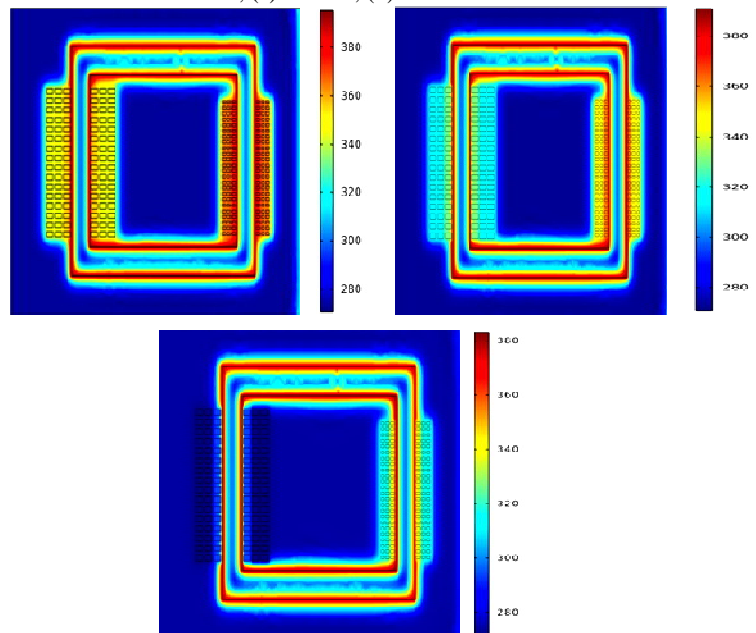


Figure 8: Temperature of hot spots in Long-time emergency regime for: (a) air; (b) MO; (c) COME; (d) PKOME

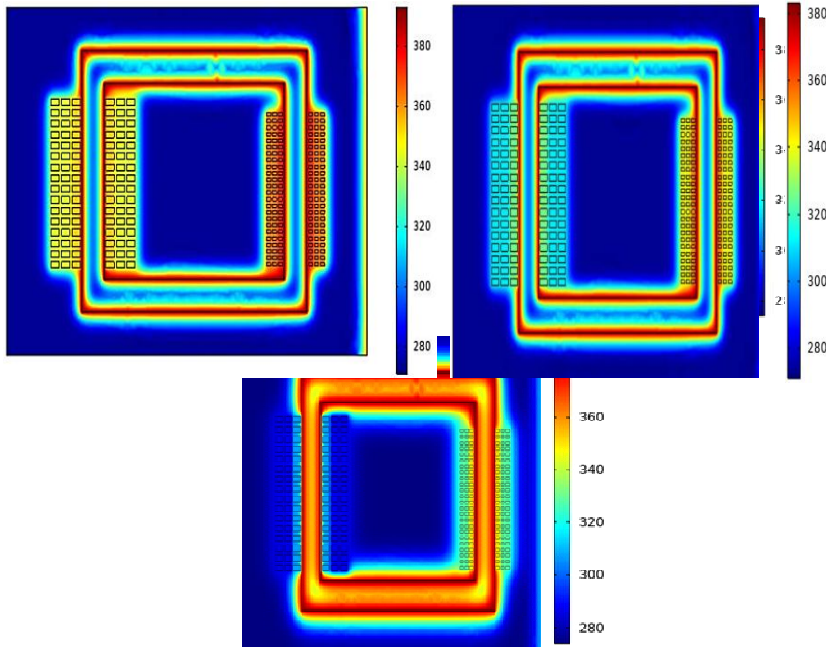


Figure 9: Temperature of hot spots in short-time emergency regime for: (a) air; (b) MO; (c) COME; (d) PKOME

Figures 7, 8, and 9 show that, the temperature distribution of hot spots increases with load. Values of the hot spot temperature are higher in air, PKOME+NANO, PKOME, and COME than in MO. Increased load contributes to increasing the maximum value of the hot spots and higher heating of the magnetic circuit and the windings. We noted that the hot spots in the above cases propagate through the magnetic circuit parts to the windings because the magnetic circuit is the most difficult part to cool down, as cooling fluids have difficulty reaching it. The same tendency is observed in the work of Kassi, Ortiz, and Fernandez [7], [8], [11]. This is because the thermal conductivity of MO and PKOME is better than that of COME and PKOME+NANO.

Using Matlab software, the evolution of the temperature of the hot spots in the transformer was plotted in each insulator for the case of the three various loads (Figure 10: 10 a, 10 b, and 10 c) as a function of time over a whole day. Table 4 gives a summary of the maximum hot-spot temperatures for air, MO, COME, PKOME, PKOME+NANO at different loads.

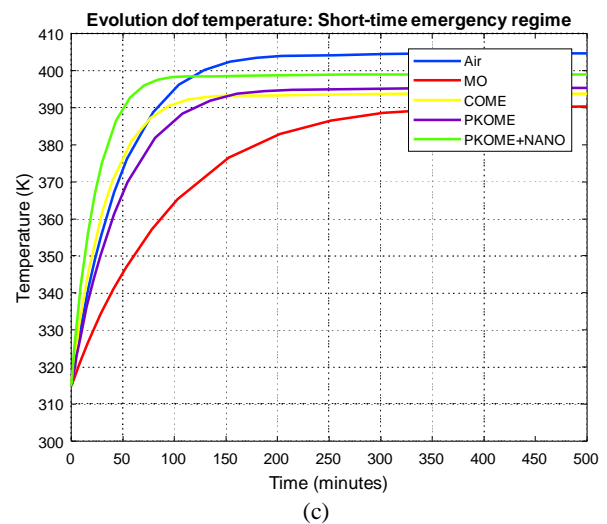
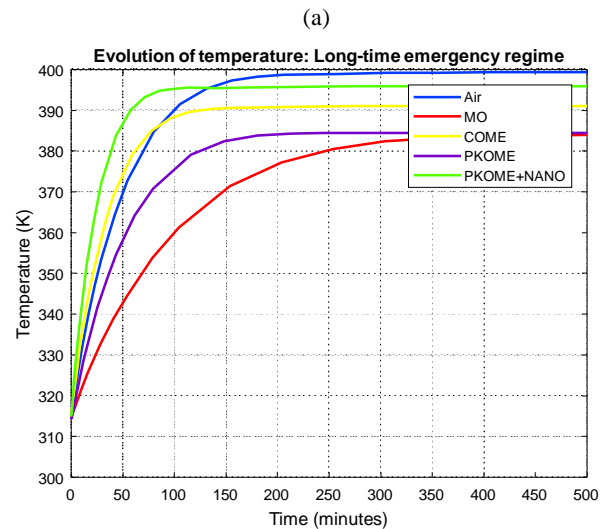
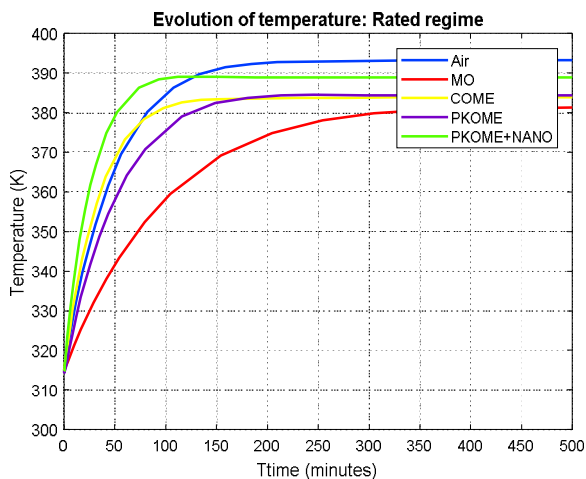


Figure 10: Temperature of hot spots: (a) rated regime; (b) long-time emergency regime; (c) short-time emergency regime

Table 4: Summary table comparing maximum temperatures of hot spots

Insulating/Dielectric Materials	Maximum temperature (K)		
	Short time emergency regime	Long time emergency regime	Rated regime
Air	404.64	399.39	393.33
MO	390.38	383.98	381.32
COME	393.72	391.07	383.87
PKOME	395.39	392.29	384.49
PKOME+NANO	398.90	395.90	389.12

The results in Figure 10 show that the value of the hot spot temperature in the transformer increases with the load over time in the different insulators. This value is a necessary element that must be measured and controlled not to exceed the limits accepted by the standard at the risk of affecting the life of the transformer. As the load increases, the transformer filled with mineral oil exceeds the maximum temperature

value set by the standard [14], which is 404.15 Kelvin for vegetable oils and 383.15 Kelvin for MO. COME, PKOME, PKOME+NANO, despite the increase of the hot spot temperature with the load, show better thermal performance than mineral oil. Because, the maximum temperature values are below the standard values as shown in Table 4. Respectively, operated in overload 393.72 K, 395.39 K, and 398.90 K for castor oil methyl ester, palm kernel oil methyl ester, and palm kernel oil methyl ester plus nanoparticles. These results have the same trend as the work of Ortiz in 2018, Mohammed in 2019, Mortaza in 2019, Kassi, and many others who also had the same conclusion with their respective esters result [7], [8], [24]. The results in Figure 7 show that the value of the hot spot temperature in the transformer increases with the load over time in the different insulators. This value is a necessary element that must be measured and controlled not to exceed the limits accepted by the standard at the risk of affecting the life of the transformer. As the load increases, the transformer filled with mineral oil exceeds the maximum temperature value set by the standard [14], which is 404.15 Kelvin for vegetable oils and 383.15 Kelvin for mineral oil. EMHR, EMHP, and EMHP+NANO.

Using these results and the relative aging rate formula, we plotted the aging curves for mineral oil and ester as shown in Figure 11. The observation confirms the results that the aging rate of an ester-filled transformer is much slower than that of a mineral oil-filled transformer concerning hot spots. This result is in line with that of Mohamed in 2020 concerning the acceleration aging of liquid in power transformer [12].

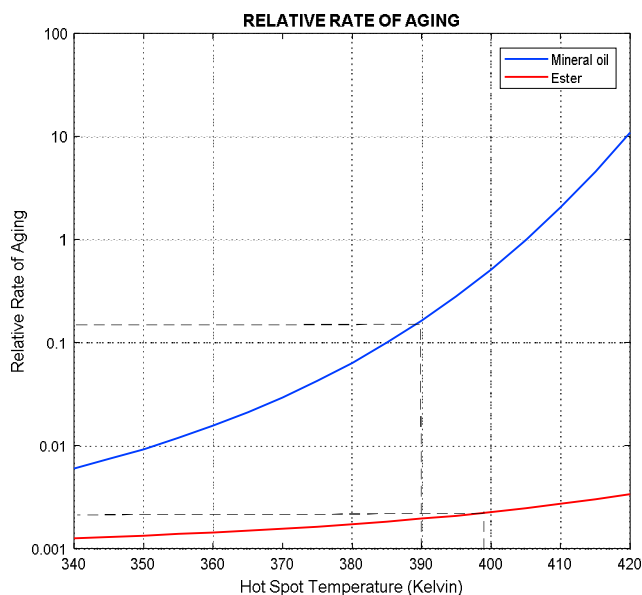


Figure 11: Relative rate of aging with hot spot temperature

5. CONCLUSION

The aim was to develop a multiphysics model of a power transformer prototype using COMSOL Multiphysics 5.4

software to perform a numerical study to evaluate the hot spot temperature distribution for each insulation (mineral oil, castor oil methyl ester, palm kernel oil methyl ester, palm kernel oil methyl ester plus titanium nanoparticles) under various loads. This was done to evaluate its thermal performance and to optimize the choice of the type of liquid insulation at the scientific level. We conclude, taking into account the result of the evolution of the temperature of the hot spots in the transformer, that the one filled with natural ester can resist more the temperature than the one filled with mineral oil (lower aging). In the following, we will use these results in the real-time experimental study of this natural ester filled prototype

REFERENCES

1. M. Talhi, I. Fofana and S.Flazi. **Impact of various stresses on the streaming electrification of transformer oil**, *Journal of electrostatics (Elsevier)*, Vol 79, pp 25-32 (2016).
2. Eleftherios I. Amoiralis, Marina A. Tsilia, Pavlos S. Georgilakis. **The state of the art in engineering methods for transformer design and optimization: a survey**, *Journal Of Optoelectronics And Advanced Materials Vol. 10, No. 5, May 2008, p. 1149 - 1158.* (2008).
3. Vasilija Sarac and Goran Cogelja. **FEM Aided Design of Distribution Transformer**, *TEM Journal* 5(2) 197–203, (2016).
4. Fernando Delgado, Alfredo Ortiz. **Study on the cooling capacity of alternative liquids in power transformers**, *IEEE Journal* (2012).
5. A. Skillen, A. Revell, H. Iacovides, W. Wu. **Numerical prediction of local hot-spot phenomena in transformer windings**, *Appl. Therm. Eng. Journal* 36 96–105 (2012).
6. T. Park and Han. **Numerical analysis of local hot-spot temperatures in transformer windings by using alternative dielectric fluids**, *Electr. Eng.* 97 (2015) 261–268.
7. R. Lecuna, F. Delgado, A. Ortiz, P.B. Castro, I. Fernandez, C.J. Renedo. **Thermal fluid characterization of alternative liquids of power transformers: a numerical approach**, *IEEE Trans. Dielectr. Electr. Insul.* 22 (2015) 2522–2529, (2015).
8. A. Ortiz, I. Fernandez, C.J. Renedo al. **The aging impact on the cooling capacity of a natural ester used in power transformers**. *Applied Thermal Engineering*, (2018).
9. Seerali Nayager. **Transformer Design Considerations Utilising Natural Ester Oils**, *College of Agriculture, Engineering and Science, University of KwaZulu-Natal*, (2018).
10. Nilakanta Meitei. **Hot Spot Detection in High Voltage Transformer by Thermal Sensor using COMSOL Multiphysics**. *IEEE Journal*, (2018).

11. K. S. Kassi. **Étude de l'impact du vieillissement des huiles minérales et alternatives sur le refroidissement des transformateurs de puissance : Approches numériques et expérimentales**, *Thèse Doctorale, l'université du québec à chicoutimi p.186. (2019).*
12. Mohamed M.M. Salama and al. **Thermal performance of transformers filled with environmentally friendly oils under various loading conditions**, *Electrical Power and Energy Systems. (2020).*
13. Kendeg Onla Clement Junior, Kenmoe Fankem Eric Duckler. **3D Multiphysics Modelling of Three-Phase Transformer**, *International Journal of Information Technology and Electrical Engineering, Volume 10, Issue 2 April 2021, (2021).*
14. IEEE Std C57.12.90-2015 (Revision of IEEE Std C57.12.90-2010). **IEEE standard test code for liquid-immersed distribution, power, and regulating transformers**, *IEEE, 2016.*
15. William Lair, Sophie Bercu. **Estimation probabiliste de la durée de vie des transformateurs à partir de la norme CEI 60076-7**. *Congrès Lambda Mu 21 " Maîtrise des risques et transformation numérique : opportunités et menaces ", Oct 2018, Reims, France. hal-02074136*
16. S G. Mengata, Adolphe Moukengue,. Juliette C. Valdemirs. **Caractérisation physicochimique de l'huile de palmiste pour utilisation dans les transformateur de distribution**, *Afrique SCIENCE vol. 11, no. 6, (2015).*
17. E. Tchamdjio Nkouetcha, G. Mengata et A. Moukengue. **Elaboration and Performance Analysis of a Bio-based Insulating Liquid from Castor Oil for Power Transformers**, *Open Access Library Journal, vol.6, no. 05, p. 1, (2019).*
18. Jean-Bernard Asse, G. Mengata Mengounou, Adolphe Moukengue Imano. **Impact of FeO₃ on the AC breakdown voltage and acidity index of a palm kernel oil methyl ester based nanofluid**, *Energy Reports, Volume 8, November 2022, Pages 275-280.*
19. ASTM. D. 4052-95, **Standard Test Method for Density and Relative Density of Liquids by Digital Density Meter**, 1995.
20. ASTM. Designation 445, **Standard Test Method for Kinematic Viscosity of Transparent and Opaque Liquids (and Calculation of Dynamic Viscosity)**, *no. Book of Standards Volume.*
21. Wen-Rong Si ,Chen-Zhao Fu and al. **Numerical Study of Electromagnetic Loss and Heat Transfer in an Oil-Immersed Transformer**, *Hindawi Mathematical Problems in Engineering Volume 2020, Article ID 6514650, 13 pages, (2020).*
22. Inmaculada Fernández, Fernando Delgado, Félix Ortiz, Alfredo Ortiz and al. **Thermal Degradation Assessment Of Kraft Paper In Power Transformers Insulated With Natural Esters**, *E.T.S. de Ingenieros Industriales y de Telecomunicación, (2011).*
23. Lakmini Wanninayaka, Chrishmal Edirisinghe, Supun Fernando, J. R. Lucas, **A Mathematical Model To Determine The Temperature Distribution Of A Distribution Transformer**, *Open Access Library Journal, 1-6, (2021).*
24. Morteza Mikha-Beyranvand, Jawad Faiz, Behrooz Rezaeealam, Afshin Rezaei-Zare. Mehrdad Jafarboland. **Thermal analysis of power transformers under unbalanced supply voltage**, *IET Electric Power Applications E-First on 15th March 2019.*